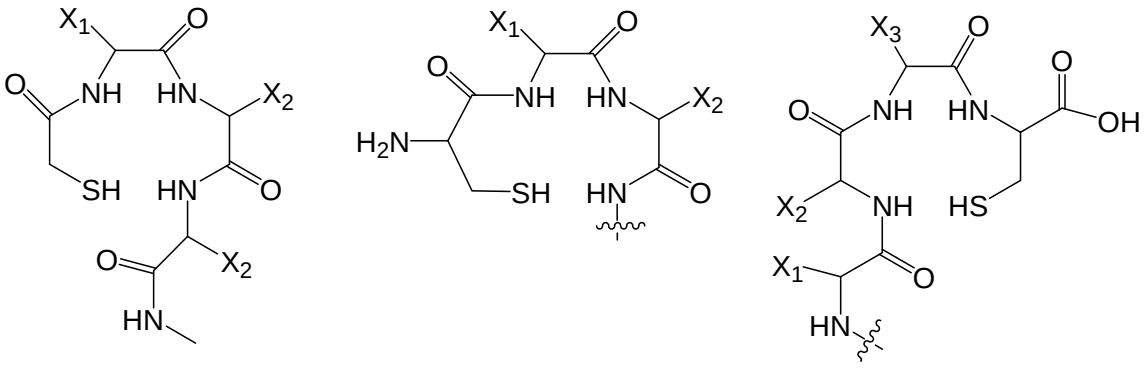

Supplemental Figure 1. Structures of various peptide-based chelators, evaluated in earlier studies of ^{99m}Tc-labeled Affibody molecules.

1. meracaptoacetyl-based chelators positioned at the N-terminus or K^{49}. maGGG: $X_1=X_2=X_3=G$; maSSS: $X_1=X_2=X_3=S$; maEEE: $X_1=X_2=X_3=E$; maESE: $X_1=E$, $X_2=S$, $X_3=E$; maEES: $X_1=X_2=E$, $X_3=S$; maSEE: $X_1=S$, $X_2=X_3=E$; maSKS: $X_1=S$, $X_2=K$, $X_3=S$; maKKK: $X_1=X_2=X_3=K$;

2. Cysteine-based chelators positioned at the N-terminus: CGG: $X_1=X_2=G$; CGG:

3. Cysteine-based chelators positioned at the C-terminus: VDC: $X_1=K$; $X_2=V$; $X_3=D$; GSECG: $X_1=G$; $X_2=S$; $X_3=E$. The cysteine is connected to glycine by an amide bond.

Influence of peptide based chelators on the distribution of radioactivity in mice after the injection of ^{99m}Tc-labeled $Z_{HER2:342}$ Affibody molecule and its derivatives

The data concerning the influence of peptide based chelators on the distribution of radioactivity in mice after injection of ^{99m}Tc-labeled $Z_{HER2:342}$ Affibody molecule and its derivatives are summarized in **Supplemental Table 1**.

The use of $[^{99m}Tc(CO)_3]^+(H_2O)_3$ for labeling of His_6-$Z_{HER2:342}$ and His_6-$(Z_{HER2:4})_2$ provided stable attachment of the radionuclide, but was associated with a high liver uptake (*12*, *23*). Later studies (*19, 22*) demonstrated that the presence of an N-terminal hexahistidyl tag was the reason for the elevated hepatic uptake. Translocation of the hexahistidyl tag to the C-terminus reduced the hepatic uptake two-fold, and the substitution of three histidines with

glutamate caused a ten-fold reduction of the hepatic uptake in murine models (*23*). However, the renal retention of radioactivity was high for all conjugates labeled using $[^{99m}Tc(CO)_3]^+(H_2O)_3$ (*23*).

Mercaptoacetyl-containing synthetic Affibody molecules seemed promising for labeling with ^{99m}Tc, but required thorough optimization of the amino acid composition of the chelating sequence. The initial use of a mercaptoacetyl-glycyl-glycyl-glycyl sequence at the N-terminus as a chelator provided reasonably good tumor targeting and low renal uptake of radioactivity, but was associated with a high level (up to 30%) of hepatobiliary excretion (*13*). By increasing the hydrophilicity of the chelating moiety, i.e. by exchanging the glycyl for seryl in the chelating sequence (maSSS chelator), the hepatobiliary excretion was reduced 3-fold, but at a cost of elevated renal retention of the radioactivity (*14*). The use of the charged amino acid glutamyl instead of the polar seryl in the maEEE chelator decreased the hepatobiliary excretion to acceptable levels, but further increased the renal retention (*16*). Although high renal uptake is considered to be more acceptable than high levels of hepatobiliary excretion, efforts were made to reduce the renal uptake by optimizing the chelator composition. It was found that a combination of seryl with glutamyl or lysyl in the mercaptoacetyl-containing chelators (*17*, *18*) provided low levels of hepatobiliary excretion, good tumor targeting and an acceptable level of renal retention. Furthermore, it was shown that the low level of renal radioactivity associated with ^{99m}Tc-maESE-$Z_{HER2:342}$ was due to the efficient clearance of renal radiocatabolites (*17*). These studies demonstrated that modification of the amino acid composition of peptide-based chelators provides an opportunity to modify the biodistribution of ^{99m}Tc-labeled Affibody molecules.

In addition, cysteine-containing peptide-based chelators were evaluated for the labeling of recombinantly produced Affibody molecules. Affibody molecules with the N-terminal chelating sequence cysteyl-glycyl-glycyl-glycyl- or cysteyl-glycyl-glycyl were labeled with ^{99m}Tc and evaluated in vivo (*15*). Specific imaging of HER2 expressing xenografts was demonstrated, but the conjugates suffered from an undesirable level of hepatobiliary excretion (~10%) and a certain degree of ^{99m}Tc-pertechnetate release in vivo. The C-terminal positioning of the cysteine allows for a more stable "XXC"-type chelator (**Figure 1**) as previously demonstrated for scFv fragments (*24*) and peptides (*25*). In a XXC technetium complex, the N_3S ligand set forms a stable chelate with three 5-member rings when complexing the technetium. When the cysteine is located at the N-terminus (CXX), metal complexation through the cysteine yields a 6-member ring in the chelate, which is known to give a less stable technetium (V) complex (*26*). To test this approach, an Affibody molecule, $Z_{HER2:2395}$ ([Ala^1,Glu^2,Thr^{23},Val^{59},Asp^{60},Cys^{61}]$Z_{HER2:342}$), having a C-terminal cysteine was labeled with ^{99m}Tc (*19, 27*). Biodistribution studies demonstrated that 1) the use of an N_3S chelator at the C-terminus provided much lower release of ^{99m}Tc-pertechnetate in comparison to the SN_3 chelator at the N-terminus; 2) placement of Ala^1,Glu^2 - at the N-terminus is associated with low hepatic uptake and low levels of hepatobiliary excretion; 3) ^{99m}Tc-$Z_{HER2:2395}$ provides efficient targeting and high-contrast imaging of HER2-expressing xenografts; 4) the renal accumulation was high (190% IA/g at 4 h pi), and it would thus be desirable to reduce it. Further studies confirmed that the composition of the N-terminus is essential for low levels of hepatic uptake, while modification of the C-terminus is less critical (*22, 20*). This indicates that keeping Ala^1,Glu^2 - at the N-terminus would provide low hepatic uptake of the Affibody molecules, while modification of the C-terminal cysteine-containing peptide based chelators might enable modulation of the renal retention of radioactivity. This concept was tested using an Affibody construct designated as PEP05352

([Ala^{1},Glu^{2},Ala^{1},Tyr^{5},Ala^{6},Thr^{23},Ser^{42},Glu^{43},Ser^{54},Gly^{56},Ser^{57},Glu^{58},Cys^{59},Gly^{60}]$Z_{HER2:342}$) (*21*). The construct was designed to enable both efficient peptide synthesis and recombinant production. In order to create an N_3S chelator at the C-terminus, an amino acid sequence – SECG (a mirror of mercaptoacetyl-glutamyl-seryl-glutamyl) was introduced. The ^{99m}Tc-PEP05352 demonstrated good targeting and stability in vivo and the renal retention was nearly 5-fold reduced in comparison with ^{99m}Tc-$Z_{HER2:2395}$. Still, this could not be considered as a strict proof of concept since a number of other modifications were introduced in the scaffold portion of PEP05352 to facilitate peptide synthesis.

Supplemental Table 1

			Uptake at 4 h after injection, %IA/g				
Construct	Chelator	Position	Blood	Liver	Kidney	Intestines with content *	Reference
H_6-$(Z_{HER2:4})_2$	H_6	N-terminus	0.54 ± 0.04	6.97 ± 0.28	89 ± 10		12
H_6-$Z_{HER2:342}$	H_6	N-terminus	0.19 ± 0.06	10 ± 3	92 ± 23	1.9 ± 0.2	23
$Z_{HER2:342}$- H_6	H_6	C-terminus	0.9 ± 0.4	5 ± 1	100 ± 16	2.5 ± 0.6	23
HEHEHE -$Z_{HER2:342}$	HEHEHE	N-terminus	0.28 ± 0.04	0.9 ± 0.2	80 ± 4	3 ± 2	23
maGGG- $Z_{HER2:342}$	maGGG [a]	N-terminus	0.13±0.01	0.66±0.16	5.98±1.14	30±11	13
maSSS- $Z_{HER2:342}$	maSSS [a]	N-terminus	0.15±0.01	0.47±0.05	33±2	11±1	14
maEEE-$Z_{HER2:342}$	maEEE [a]	N-terminus	0.21±0.04	0.51±0.07	104±14	3.6±0.9	16
maESE-$Z_{HER2:342}$	maESE [a]	N-terminus	0.17±0.03	0.33±0.06	33±5	2.4±0.4	17
maEES-$Z_{HER2:342}$	maEES [a]	N-terminus	0.24±0.11	0.90±0.31	68±21	4.1±1.2	17
maSEE-$Z_{HER2:342}$	maSEE [a]	N-terminus	0.16±0.03	0.48±0.07	71±10	1.9±0.3	17
maSKS- $Z_{HER2:342}$	maSKS [b]	N-terminus	0.15±0.02	0.6±0.2	33±2	4.3± 0.5	18
maKKK- $Z_{HER2:342}$	maKKK [b]	N-terminus	0.23 ± 0.01	7 ± 2	127± 9	4.0 ±0.3	18
$N^{\varepsilon 49}$-maSSS- $Z_{HER2:342}$	maSSS	K^{49}	0.20±0.02	0.86±0.08	48.6±0.8	5.38±0.60	20
$N^{\varepsilon 49}$-maESE-$Z_{HER2:342}$	maSSS	K^{49}	0.22±0.05	0.39±0.08	17±5	3.05±0.51	20
CGG- $Z_{HER2:342}$	CGG- [b]	N-terminus	0.8 ± 0.2	1.3± 0.2	59 ± 9	17.1 ± 0.8	15
H_6-$Z_{HER2:342}$-C	-VDC [b]	C-terminus	0.12±0.01	6.1±1.3	103±31	2.5±0.6	19
$Z_{HER2:2395}$	-VDC [c]	C-terminus	0.08±0.02	1.5±0.2	191±15	1.5±0.3	19
PEP05352	-GSECG [c]	C-terminus	0.21±0.02	1.5±0.2	48±6.	1.9±0.10	21

*data for intestines with content (estimate of hepatobiliary excretion) are presented as %IA/whole sample.
[a] Balb/C nu/nu mice bearing SKOV-3 xenografts;
[b] NMRI mice
[c] Balb/C nu/nu mice bearing LS174T xenografts;

$Z_{HER2:2395}$ = [Ala^1,Glu^2,Thr^{23},Val^{59},Asp^{60},Cys^{61}]$Z_{HER2:342}$;
PEP05352 =[Ala^1,Glu^2,Ala^1,Tyr^5,Ala^6,Thr^{23},Ser^{42},Glu^{43},Ser^{54},Gly^{56},Ser^{57},Glu^{58},Cys^{59},Gly^{60}]$Z_{HER2:342}$

Supplemental Table 2. Biodistribution of ^{99m}Tc-labeled Affibody molecules in male NMRI mice after intravenous injection. The uptake is expressed as % IA/g and presented as an average value from 4 animals ± standard deviation.
* data for intestines with content and carcass are presented as % of injected radioactivity per whole sample

Uptake, 1 h pi					
conjugate	^{99m}Tc-$Z_{HER2:V1}$	^{99m}Tc-$Z_{HER2:V2}$	^{99m}Tc-$Z_{HER2:V3}$	^{99m}Tc-$Z_{HER2:V4}$	^{99m}Tc-$Z_{HER2:V5}$
C-terminus	GSEC	GGGC	GGSC	GGES	GGKC
blood	1.2±0.1	1.4±0.5	1.1±0.2	1.0±0.2	0.8±0.2
lung	1.7±0.1	2.1±0.4	1.4±0.2	3.0±1.0	1.7±0.3
liver	1.5±0.1	2.1±0.4	2.2±0.4	1.7±0.1	4.4±0.5
spleen	0.48±0.09	0.9±0.1	0.8±0.2	0.6±0.1	1.0±0.2
stomach	0.9±0.1	1.2±0.	0.9±0.2	0.89±0.2	0.90±0.14
kidney	81±15	24±6	94±8	132±13	139±10
salivary gland	0.7±0.1	0.6±0.2	1.0±0.7	0.6±0.1	0.49±0.07
muscle	0.38±0.03	0.95±0.97	0.4±0.1	0.5±0.3	0.38±0.04
intestines*	1.9±0.4	2.8±0.4	1.7±0.4	2.5±0.7	2.6±0.5
carcass*	11.6±0.6	11.7±2.6	11.7±2.7	12.0±2.0	12.2±2.3
Uptake, 4 h pi					
blood	0.15±0.03	0.13±0.04	0.13±0.03	0.16±0.02	0.13±0.01
lung	0.3±0.1	0.4±0.1	0.35±0.06	1.01±0.4	1.06±0.15
liver	0.87±0.05	0.83±0.06	1.1±0.1	1.1±0.2	3.3±0.1
spleen	0.13±0.01	0.22±0.05	0.24±0.05	0.23±0.08	0.88±0.08
stomach	0.28±0.04	0.20±0.08	0.23±0.03	0.5±0.2	0.49±0.06
kidney	19±5	6.4±0.6	15±4	27±4.0	120±9
salivary gland	0.20±0.06	0.08±0.02	0.13±0.04	0.18±0.07	0.27±0.06
muscle	0.09±0.04	0.09±0.04	0.10±0.06	0.2±0.2	0.14±0.02
intestines*	1.2±0.3	1.7±0.6	2.2±0.9	3.3±1.0	2.4±0.3
carcass*	2.2±0.3	1.6±0.2	2.9±0.7	4.2±1.0	5.1±0.2
Uptake, 24 h pi					
blood	0.012±0.001	0.02±0.004	0.021±0.004	0.013±0.002	0.040±0.002
lung	0.05±0.02	0.12±0.04	0.08±0.02	0.08±0.01	0.25±0.03
liver	0.17±0.03	0.3±0.1	0.21±0.02	0.14±0.04	0.80±0.09
spleen	0.042±0.008	0.12±0.05	0.071±0.008	0.05±0.02	0.27±0.001
stomach	0.09±0.04	0.07±0.02	0.053±0.006	0.032±0.004	0.16±0.04
kidney	5±1	1.6±0.5	1.20±0.09	1.0±0.2	15.3±3.5
salivary gland	0.031±0.009	0.026±0.008	0.03±0.02	0.017±0.003	0.07±0.01
muscle	0.008±0.001	0.009±0.002	0.014±0.006	0.006±0.002	0.034±0.002
intestines*	0.6±0.5	0.2±0.1	0.17±0.05	0.29±0.17	0.44±0.07
carcass*	0.41±0.06	0.4±0.1	0.9±0.6	0.41±0.02	1.22±0.04